30th Congress of the International Council of the Aeronautical Sciences
DCC, Daejeon, Korea ; September 25-30, 2016

THE MANUFACTURE AND APPLICATION FOR COMPOSITES AEROELASTIC MODEL OF CIVIL AIRLINER WING IN FL-26 TRANSONIC WIND-TUNNEL

Zibin Yan*, Wei Qian, Rui Yang*, Xianjun Sheng*****
***School of Mechanical Engineering, Dalian University of Technology**
****School of Aeronautics and Astronautics, Dalian University of Technology**
*****College of Electronic Science and Technology, Dalian University of Technology**

Keywords: *Composites, aeroelastic scaled model, airliner wing, wind-tunnel test, manufacture*

Abstract

An aeroelastic model of civil airliner wing is designed and manufactured in purpose of studying the physical phenomenon of aeroelasticity, and the corresponding calculation method is tested after the wind-tunnel test. The stiffness feature of scaled model is designed by providing similar matrices of elastic influence coefficients. Suitable structural design and material choice are optimized. In addition, the objective matrices of elastic influence coefficients of wing are provided with acceptable precision. The precision of static-aeroelastic feature of scaled model is ensured by stiffness deviation calibration method during manufacture processes. The objective matrices of elastic influence coefficients are obtained by applying successive approximation method in static loading test.

1 Introduction

Static-aeroelasticity affects the outer shape of aircrafts in flight and any deformation of aerodynamic surfaces would certainly alters the aerodynamic loading. Improper static-aeroelastic design may cause losing handling stability, divergent deformation of lifting surfaces and even damages on wing surfaces[1,2]. Currently, wind-tunnel tests are used to acquire the quantitative relation between the ideal outer shape in cruise and the outer shape in flight, due to the shortage of reliable static aeroelasticity coupling simulation method. Obviously, the wind-tunnel scaled model should be manufactured with similar static-aeroelastic characteristics to the original aircrafts design.

Ever since the concept of structural design optimization was introduced into wind-tunnel scale model design process[3-6], the composites material have been studied and used in wind-tunnel scaled model manufacture because of its designability of superior mechanical performance and its high stiffness-weight ratio.

In this paper, a composites aeroelastic model of civil airliner wing used in FL-26 transonic wind-tunnel was designed and the aeroelastic similarity between the model and aircraft was ensured. This model was built using composites material and by designing the spars, truss and the corresponding composites surface stack-ups, the matrices of elastic influence coefficients (MEIC) of this model were formulated within acceptable range of similarity to the objective matrices of elastic influence coefficients. In the ground static load test, the strength of this model was proved to be sufficient while the stiffness characteristics of this model was provided with acceptable precision for wind-tunnel test.

2 The structural design of scaled model

2.1 The structural similarity principle

The scaled model used in wind-tunnel should be geometrically scaled so it could be fit into a reasonable air flow field in the wind-tunnel. Consequently, the geometrical outer shape of scaled model should be in proportional relationship to the real aircraft, and the dynamic pressure in the wind-tunnel needs to be in proportional relationship to the real flight environment.

$$k_l = L_m / L_a \quad (1)$$

$$k_q = q_m / q_a \quad (2)$$

The geometrical outer shape parameter L_m should be similar to the geometrical outer shape parameter L_a of original aeroelastic model. The dynamic pressure q_m of wind-tunnel should be similar to the dynamic pressure q_a at cruise point.

Correspondingly, the bending stiffness characteristic k_{EI} and torsional stiffness characteristic k_{GJ} could be given in proportional relationship to the original aircraft design[2].

$$k_{EI} = k_q k_l^4 \quad (3)$$

$$k_{GJ} = k_q k_l^4 \quad (4)$$

2.2 The structural optimization based on MEIC approximation

This scaled model uses the concept of matrices of elastic coefficients similarity design[6]. The model alteration is completed based on the simplified finite element model (FEM) of original aircrafts.

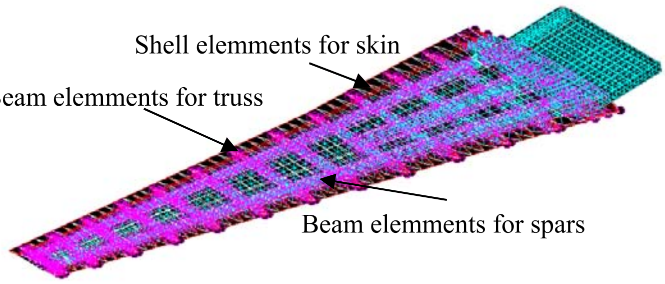

Fig. 1 The Finite Element Model of Aeroelastic Scaled Model

Tab. 1 The Mechanical Performance of Model Material

Model parts	Material	Elastic modulus (Gpa)	Possion Ratio	Density (Kg/m^3)
Spar	Glass fiber/ epoxy resin	11	0.22	2540
Truss	Glass fiber/ epoxy resin	11	0.22	2540
Skin	Carbon fiber/ epoxy resin	120	0.31	1620
Filling foam	RC 200WF	0.27	0.33	205

In FEM shown in Fig. 1, the spar and truss structure are simulated with series of beam elements and the skins of model are simulated with shell elements. In this model, the spar and truss in aeroelastic scaled model is made of several kinds of composites, whose physical performance is given in Table. 1. Mechanical performance of these material were acquired through tensile test (shown in Fig. 2).

Obviously, the structural design of scaled model could be concluded as geometrical parameters of sections and different thickness parameters of shell. What should be noted is that, to lower the calculation difficultness, the geometrical parameters were restrained to the crucial parameters of sections.

Fig. 2 The tensile test of the composites material

The matrices of elastic influence coefficients (MEIC) of scaled model composed of geometrical parameters θ_i, r_i and t_i could be obtained. MEIC can be calculated as:

$$W = XG^{-1}X^T \tag{5}$$

Here G is the assembled stiffness matrix in polynomial coordinates; X is the transformation matrix from vector of assembled polynomial coordinates u to physical displacements w in specified M points ($w=Xu$)[6].

While the MEIC of scaled model should be in proportional relationship to the MEIC of aircraft. The design principles of this model is given[6].

$$\varepsilon_1 = \frac{1}{n}\sum_{i=1}^{n}\left|1 - W_{ii}/W_{ii}^m\right| \qquad i = 1,2,\cdots n \tag{6}$$

$$\varepsilon_2 = \frac{1}{n^2}\sum_{i=1}^{n}\sum_{j=1}^{n}\left|1 - W_{ij}/W_{ij}^m\right| \qquad i = 1,2\cdots n \tag{7}$$

$$\varepsilon_3 = \max\left(\left|W_{ij} - W_{ij}^m\right|\right)/\max\left(\left|W_{ij}^m\right|\right) \qquad i = 1,2\cdots n \tag{8}$$

$$\varepsilon_4 = \sum_{i=1}^{n}\sum_{j=1}^{n}W_{ij}\Big/\sum_{i=1}^{n}\sum_{j=1}^{n}W_{ij}^m - 1 \qquad i = 1,2\cdots n \tag{9}$$

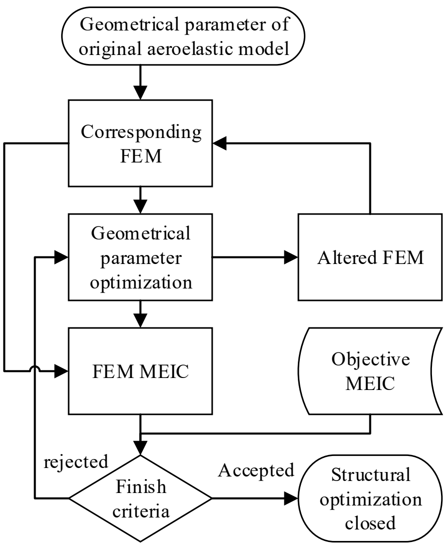

Fig. 3 The flow chart of geometrical parameters optimization

The optimization flow chart is given in Fig. 3. In purpose of forming a suitable geometrical parameters solution, the corresponding optimization based on discrete model is shown. In this optimization, the structural material used are predesigned to show isotropic mechanical performance.

$$\left\{\begin{array}{ll} \min & f(\theta_p, r_q, t_s) = (\varepsilon_k)^2 \\ & \varepsilon_1 = \frac{1}{n}\sum_{i=1}^{n}\left|1 - W_{ii}/W_{ii}^m\right| \\ & \varepsilon_2 = \frac{1}{n^2}\sum_{i=1}^{n}\sum_{j=1}^{n}\left|1 - W_{ij}/W_{ij}^m\right| \\ & \varepsilon_3 = \max\left(\left|W_{ij} - W_{ij}^m\right|\right)/\max\left(\left|W_{ij}^m\right|\right) \\ & \varepsilon_4 = \sum_{i=1}^{n}\sum_{j=1}^{n}W_{ij}\Big/\sum_{i=1}^{n}\sum_{j=1}^{n}W_{ij}^m - 1 \\ s.t. & g(x) = \varepsilon_m \quad m \neq k \\ & 0 < \theta_p < \overline{\theta}_P \\ & 0 < r_q < \overline{r}_Q \\ & 0 < t_s < \overline{t}_S \\ & i = 1,2,\cdots n \\ & j = 1,2,\cdots n \\ & k = 1/2/3/4 \end{array}\right. \tag{10}$$

Ideally, an engineering optimization method is used, by computing the sensitivity of design variables to the objectives using the method of finite difference, the optimization plan could be deployed, and corresponding optimization algorithm could be used.

What should be noted is that the mechanical performance of material used in this optimization show isotropic mechanical performances, so the composites used to build the scaled model need to be designed to present similar mechanical performances. Currently, the composites stack-ups used are symmetric laminates like [0° / 45° / 90° / -45° / 0°], and this kind of stack-ups is used for shell thickness t_s. The final structural design of this model is presented in Fig. 5.

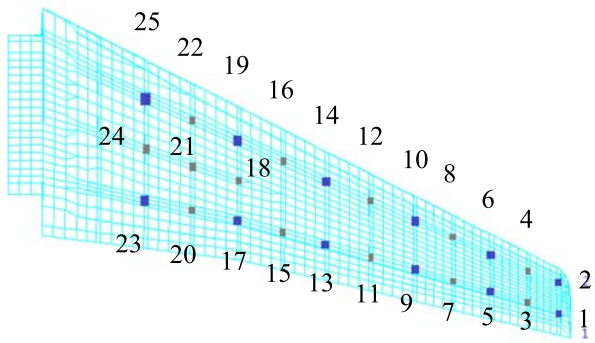

Fig. 4 Testing points on scaled model

Tab. 2 The stiffness error between FEM after design and objective FEM

Test point	error	Test point	error
1	-12.24%	13	1.36%
2	-11.77%	14	0.98%
5	1.21%	17	0.21%
6	0.42%	19	-0.43%
9	2.47%	23	-11.12%
10	2.07%	25	8.13%

The stiffness k_i of test point i is acquired by applying unit load F_{i1} on that point, and record the displacement d_i on that point.

$$k_i = F_{i1} / d_i \qquad (11)$$

The FEM after design process is compared to the objective FEM. The test point is shown in Fig. 4, and the stiffness error is shown in Tab. 2.

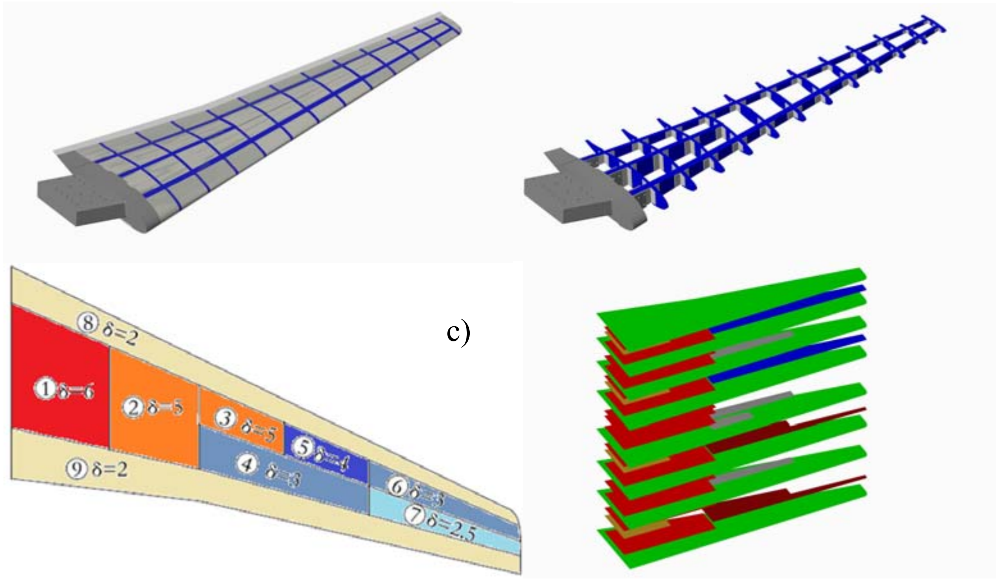

Fig. 5 The structural design after optimization
a) The scaled model. b) Spars and truss. c) Partitions of different thickness on model. d) The stack-ups of composites.

3 The manufacture of static-aeroelastic scaled model

3.1 The manufacture problem of scaled model

The manufacture of this scaled model is different from normal products, because the composites material composed of reinforced fiber and epoxy resin show high disparity in mechanical performance. A scaled model made of composites using traditional manufacture routine could lead to error from the ideal mechanical characteristics, in addition, the carbon fiber/epoxy resin composites material could hardly be processed with normal processing method, because even the geometrical parameters of this model could be provided with acceptable precision, there will be potential structural failure caused by mechanical processing. This would certainly affect the safety of wind-tunnel test. Due to the instability of the composites mechanical performance after curing process, a predesigned, geometrically constrained manufacturing routine may not be applicable. To build a scaled model with acceptable mechanical performance precision and dynamical performance precision, a performance-oriented manufacturing routine should be used. Furthermore, to eliminate potential structural failure caused by mechanical processing, the fabrication of composites should be an additive process.

3.2 The manufacture process of scaled model

To manufacture a scaled model with little potential structural failure and acceptable stiffness precision, a specially designed manufacture routine is presented (shown in Fig. 6).

Before manufacture, the structural design of scaled model was studied and several layers of (carbon fiber/ epoxy resin) were replaced with (glass fiber/ epoxy resin). Because the stiffness/weight ratio of carbon fiber was bigger than the one of glass fiber, so the stiffness of scaled model was lowered.

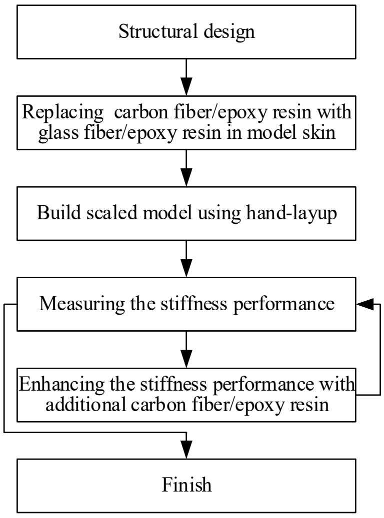

Fig. 6 The manufacture routine of scaled model

Furtherly, a scaled model of lower stiffness was built using hand-layup method (shown in Fig. 7).

Fig. 7 The scaled model in hand lay-up process

After building a scaled model with lower stiffness, the actual stiffness of this model was tested so the gap ΔF to the ideal stiffness could be acquired.

Furthermore, the stiffness of model could be enhanced by adding additional carbon fiber / epoxy resin layers on the inner surface of model skin.

In formula (12), the stiffness f_c is composed of several parameters showing manufacturing convenience. ES_{ei} and ES_{gj} indicate the upper limit of model material mechanical performance parameters and geometrical parameters while EI_{ei} and EI_{gj} indicate the lower limit of model material mechanical performance parameters and geometrical parameters.

$$\begin{cases} obj: \quad \min\{\Delta F - f_c(e_i, g_j)\} \\ s.t. \quad ES_{ei} \ge e_i \ge EI_{ei} \\ \qquad ES_{gj} \ge g_j \ge EI_{gj} \\ \qquad i = 1,2,3,\cdots,M \\ \qquad j = 1,2,3,\cdots,L \end{cases} \tag{12}$$

In formula (12), the geometrical parameter g_j and mechanical performance of specified material e_i are the design variables. The number of e_i is M and the number of g_j is L.

The stiffness enhancing design could be acquired after this optimization. Corresponding structural optimization like topological optimization or geometrical dimension optimization could be used to formulate reasonable enhancing solution.

4 The ground test of scaled model

4.1 The static-loading test of scaled model

Before static-aeroelastic test in FL-26 wind-tunnel, a static-loading test was conducted, so the static-elastic performance and strength of this scaled model bearing aerodynamic loads could be tested. The aerodynamic load was simulated with multiple tensile loads on the surface of the scaled model, and the static load was generated using a hydraulic cylinder. The static load was applied using 6 fixtures, which is shown in Fig. 9. Furtherly, the static load was applied in a loading process shown in Fig. 11. During the test, the deformation of the scaled model was tested using displacement sensors attached to the surface of the scaled model.

Fig. 8 The Installation of scaled model

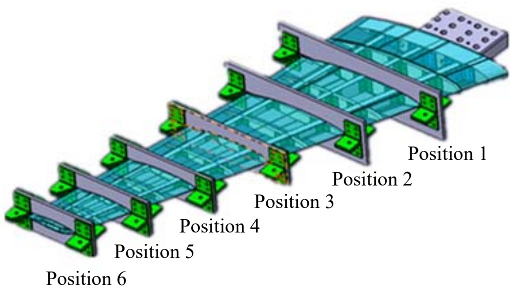

Fig. 9 The testing positions and fixtures

In Fig. 8, the scaled model was fixed on a base, and a progressively increasing load was applied using several loading devices.

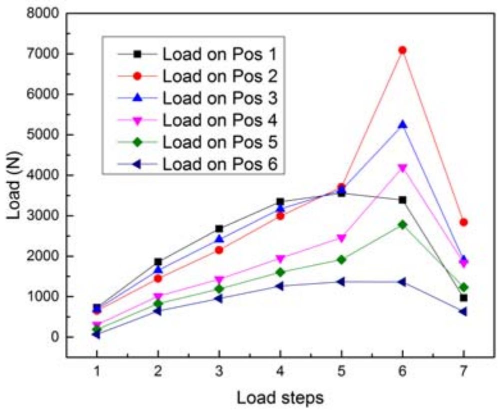

Fig. 10 The loading process at position 1~6

In Fig. 10, the loading processes on position1~6 are presented. During this loading process, the aerodynamic loads are applied with progressive increases at each loading position. At position 6, the general tensile load on scaled model is 24049.8N. During this loading process, the deformation measured by displacement sensors shows elastic deformation result, and the strain on the wing surfaces are within the safety range. All these indicate that the static-strength of this scaled model is strong enough for static aerodynamic load of 25000N.

4.2 The stiffness test of scaled model

In purpose of studying the static-elastic performance of scaled model, a static loading process was applied. The static loads on the model surfaces were measured using force sensors and the displacements of test points were measured using displacement sensors. The stiffness of scaled model was acquired by linear fitting the data collected.

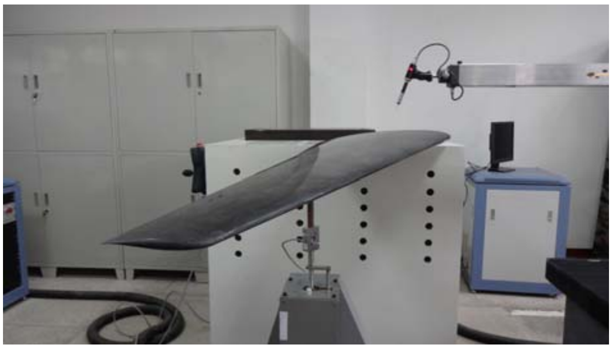

Fig. 11 The stiffness test of scaled model

Tab. 3 The stiffness error between scaled model in test and objective FEM

Test point	error	Test point	error
1	-4.37%	**11**	-2.37%
2	-1.83%	**12**	5.86%
3	2.08%	**15**	-5.30%
4	5.36%	**16**	5.21%
7	1.38%	**20**	-9.72%
8	5.69%	**22**	6.00%

The stiffness error of several points (shown in Fig. 4) between the scaled model and the objective FEM are presented in Tab. 3.

4.3 The natural frequency and mode of scaled model

The modal characteristics of this scaled model were tested by applying transient excitation on the scaled model, then the acceleration responses on several points were collected. The modal characteristics were acquired by applying modal identification method. Simultaneously, the modal characteristics of the objective FEM of the scaled model were acquired through finite elements analysis. The cloud images of mode displacement of several modes are given in Fig. 12~15. The difference of natural frequency between scaled model and FEM are given in Tab. 4.

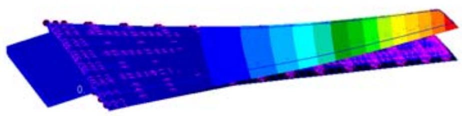

Fig. 12 The 1st bending mode of scaled model

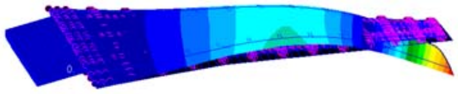

Fig. 13 The 2nd bending mode of scaled model

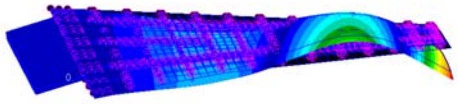

Fig. 14 The 3rd bending mode of scaled model

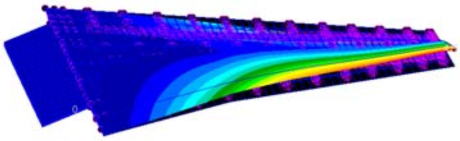

Fig. 15 The 1st torsional mode of scaled model

In Fig. 12, the 1st bending mode of scaled model is shown, and the 2nd bending mode and 3th bending mode is shown in Fig. 13 and Fig. 14. The 1st torsional mode is presented in Fig. 15.

The error of natural frequencies of bending mode and torsional mode between the scaled model and the objective FEM are presented in Tab. 4.

Tab. 4 The natural frequency error between scaled model after enhancing and objective FEM

1st bending	2nd bending	3rd bending	1st torsion
4.97%	3.29%	1.01%	-0.76%

5 Conclusion

The wind-tunnel tests are established to acquire the quantitative relationship between the ideal outer shape in cruise and the outer shape in flight. The scaled model used in wind-tunnel test could provide aeroelastic performance similar to the actual aircrafts. In this paper, a scaled model of civil airliner wing was manufactured concerning the similarity of MEIC between the scaled model and objective design.

In the static loading test presented in section 4, this scaled model was proved to be strong enough to bear static load of 24049.8N. This result shows that the scaled model is strong enough for the static-aeroelastic test in FL-26 wind tunnel.

The stiffness error between the scaled model and objective FEM are less than 10%, and most stiffness error are less than 6%. This result proves that the scale model is manufactured with acceptable MEIC precision.

Corresponding modal test result proved that the modal characteristics of this model show acceptable precision. The natural frequency error of 1~3th bending mode and 1st torsional mode are less than 5%. The dynamical similarity relationship between the model and actual aircrafts are provided with acceptable precision.

Above all, this scaled model present similar static-elastic characteristics and dynamical performance to the objective FEM, the strength of this model is proved to be sufficient for wind-tunnel test. So this scaled model is proved to be solid for experimental use.

Besides, there are several facts should be noted.

1) The stiffness error on the wing tips and the connector sides are more significant than the other points. The lower stiffness on the connector sides could be a result of the bad connection between the skin parts and the spar parts, and the bad connection between the connector and the truss could leave gaps which would certainly lead to lower stiffness. The error of bigger stiffness error could be a result of small resin volume fraction in composites.

2) To acquire detailed mechanical characteristics along with more accurate mass distribution, a specified mechanical characteristics and physical characteristics identification method should be applied, and this would certainly provide usable target for further dynamical performance calibration.

6 Contact Author Email Address

yzb@mail.dlut.edu.cn

7 Acknowledgement

This work was supported by the National Natural Science Foundation of China (Grant No. 51275073).

Copyright Statement

References

[1] W. Faxiang. *High speed wind tunnel testing*. National Defense Industry Press, 2003.

[2] Y. Qilin. *Experiments in aerodynamics*. National Defense Industry Press, 1991.

[3] F. Mark and F. Eastep. Aeroelastic model design using parametric identification. *35th Structures, Structural Dynamics, and Materials Conference*, 1994

[4] F. Mark and E. F. *Aeroelastic model design using structural optimization*. American Institute of Aeronautics and Astronautics, 1992.

[5] M. Brian, W. Stroud, K. Thiagarajan, et al. Probabilistic design of a wind tunnel model to match the response of a full-scale aircraft. *46th AIAA/ASME/ASCE/AHS/ASC Structures, Structural Dynamics and Materials Conference*, 2005

[6] C. Vasily, I. Fanil, Z. Mikhail, et al. Optimization approach to design of aeroelastic dynamically-scaled models of aircraft. *10th AIAA/ISSMO Multidisciplinary Analysis and Optimization Conference*, 2004